



ОБЪЕДИНЕННЫЙ  
ИНСТИТУТ  
ЯДЕРНЫХ  
ИССЛЕДОВАНИЙ

Дубна

95-204

E4-95-207

V.O.Nesterenko<sup>1</sup>, W.Kleinig<sup>2</sup>

APPLICATION OF NUCLEAR THEORY METHODS  
TO NEW FAMILY OF FERMI SYSTEM

Submitted to XXIX PNPI Annual Particle and Nuclear Winter School,  
St.-Petersburg, 13—19 February 1995

<sup>1</sup>nester@thsun1.jinr.dubna.su

<sup>2</sup>On leave of absence from Technical University Dresden, Institute for  
Analysis, Dresden, Germany  
kleinig@thsun1.jinr.dubna.su

1995

# 1 Introduction

Due to a remarkable progress in experimental techniques, the new family of small Fermi systems (SFS) (metal clusters, fullerenes, helium clusters and quantum dots) was discovered about ten years ago. As was established, these Fermi systems have a striking similarity with atomic nuclei (see reviews and conference proceedings [1-9]). The most remarkable feature of new SFS is that they possess a mean field of the same kind as in atomic nuclei which allows one to investigate SFS by nuclear theory methods. If recent investigations of SFS have mainly been limited to atoms and atomic nuclei, our present possibilities have become much wider. We have really obtained a good chance for studying both a common behavior of SFS and a wonderful variety of their properties.

In the present paper, the particular properties of the new SFS as well as the application of nuclear physics methods to their description are briefly reviewed. The properties of the new SFS and atomic nuclei are continually compared. The main attention is paid to metal clusters (MC) or, more precisely, to  $E\lambda$  giant resonances (GR) in this system. In Sec.2, the sketch of basic properties of MC as well as the perspectives of their investigation are given. Sec.3 is devoted to the description of  $E\lambda$  GR in MC. In Sec.3 the properties of fullerenes, helium clusters and quantum dots are outlined. In Sec.4 the conclusions are presented.

## 2 First description of MC

MC are bound systems consisting of atoms of certain metals. We will consider here MC composed from atoms of alkali metals (sodium, potassium etc.). In alkali metals, valence electrons are *weakly* coupled with the ions and thus are not strongly localized in space, like nucleons in atomic nuclei. The mean path of valence electrons is of the same order of magnitude as the size of MC. As a result, there are good conditions for forming in MC a mean field of the same kind as in atomic nuclei. Valence electrons can be considered as counterparts on nucleons in a nucleus. Just valence electrons determine the quantum properties of MC.

It is convenient to regard a cluster as a system of valence electrons in a field of positively charged ions. For alkali metals the ion lattice can, to good accuracy, be replaced by a uniform distribution of the positive charge over cluster's volume (jellium approximation). The ionic jellium is "frozen", i.e. has no any intrinsic excitations. The jellium approximation greatly simplifies an investigation of MC. It works best for sodium clusters where the coupling of valence electrons with ions is especially weak.

Some basic characteristics of MC are presented below (in atomic units of energy, 1 a.u.=  $2Ry = 27.2$  eV, and length, 1 a.u.=  $\hbar^2/mc^2 = 0.529\text{\AA} = 0.529 \cdot 10^{-10}m$ ). The MC radius is given by  $R = r_{WS} \cdot N^{1/3}$ . Here, N is the number of atoms in the cluster;  $r_{WS}$  is the Wigner - Seitz radius that is connected with the bulk density  $n^+$  by the expression  $n^+ = (4/3\pi r_{WS}^3)^{-1}$ . In what follows, we will mainly consider sodium clusters. For sodium,  $r_{WS} = 3.93$  a.u. and the radii of sodium clusters with  $N=20-200$  are between  $5.6 - 12.2$   $\text{\AA}$ . The ionization potential (the minimal energy to remove an electron from MC) of a sodium cluster is  $3-4.5$  eV. Sodium atom is monovalent. So, in sodium clusters  $N = N_e$  where  $N_e$  is the number of valence electrons in the cluster.

Let us outline the perspectives of the MC studies (see reviews [3,7] and references therein).

1) MC with  $N \sim 20000$  and more have already been produced. Thus, we have now a unique chance for studying all the way from a single atom (through clusters) to a bulk.

2) Small clusters are quantum systems while large MC are more classical ones. So, MC provide a possibility for studying the transition from quantum to classical behavior of SFS.

3) About 30 shells have been discovered in MC which is much more than in nuclei and atoms. As a result, there are wide possibilities for investigation of the physical nature of quantum shells, namely, of the connection of quantum shells with their classical counterparts - periodic orbits [10]. Besides shells, the supershells have been predicted [11] and then observed experimentally [12] in MC. Supershells can exist only in sufficiently large systems ( $N > 1000$ ). It is clear that this effect is impossible in atoms and nuclei.

4) Like nuclei, MC with open shells have quadrupole deformation. The experiments have revealed both prolate and oblate spheroidal shapes, as well as  $\gamma$ -deformation. There are theoretical predictions of hexadecapole and octupole deformations in MC [13,14]. MC provide a unique chance for studying shapes of Fermi systems with a large number of particles.

5) Like nuclei, positively charged MC exhibit a spontaneous fission. Using the clusters with the charge  $Z \leq +14$ , the critical value of  $Z^2/N \sim 1/8$  has been empirically found (as compared with the value  $Z^2/N \sim 49$  in nuclei).

6) The pairing in MC, as a possible origin of the experimentally detected even-odd difference in the ionization potential (at temperature  $100-500$  K), is now discussed (see [15] and refs. therein). The discovery of pairing in MC could have far-reaching consequences as a new manifestation of high-temperature superconductivity.

7) MC are rather attractive for investigation of thermal effects. Since in MC the mass of the ions is much larger than the mass of the valence electrons, almost all thermal energy is contained in ions. As a result, valence electrons can be considered as a subsystem embedded into the thermal bath. Unlike nuclei, we have here the exact case of the canonical ensemble.

8) The E1 GR has been observed experimentally in a variety of clusters: small and large, spherical and deformed, neutral and charged. There are also theoretical predictions for E0, multipole  $E\lambda(\lambda > 1)$  and magnetic GR. However, experimental data for these GR are rather scarce and unreliable. GR in MC are discussed in detail in Sec.3.

9) MC of the mixed type, i.e., including atoms of different metals, can exist. The study of mixed MC is quite interesting in connection with possible practical applications (new alloys, etc.).

10) Since MC resemble atomic nuclei, a lot of models and approaches intensively used in nuclear theory can, after some modification, be effectively applied to studying MC. At the present time, the modified Nilsson single-particle potential (for small clusters) [5,16] and Woods-Saxon potential [11,13,14] (for both small and large clusters) are widely used. The liquid-drop model is used for investigation of fission in MC. The equilibrium deformations are calculated by Strutinsky's shell-correction method [13,14]. It is interesting that this method is more suitable for MC than for nuclei. The point is that, unlike nuclei, the Fermi level in MC is in the middle of the potential wall ( $E_{Fermi} = -3\text{eV}$ ,  $V_0 = -6\text{eV}$ ). As a result, the influence of quasi-bound single-particle levels is weaker in MC than in nuclei, which improves the accuracy of the shell-correction calculations. The BCS method as well as the particle-number-projection method are used for investigation of possible pairing effects [15]. Different approaches are applied to the description of GR in MC: the sum-rule method (SRM), the vibrating-potential model (VPM), various forms of the random phase approximation (RPA) (including the full RPA, the local RPA and the schematic RPA), different versions of the self-consistent models, large-basis shell model, interacting-boson model, fluid-dynamical models and others (see refs. in [3,7]). This is practically the same set of models which is used for studying GR in nuclei.

### 3 Giant resonances in MC

As compared with atomic nuclei, GR in MC have some important peculiarities.

1) GR represent practically a single type of collective motion which

has been observed in MC. In principle, deformed clusters can rotate. But a very large value of the moment of inertia results in very small values of rotational energies which, being of the same order of magnitude as thermal energy, are difficult to be observed.

2) Since the rotational bands are not observed in MC, the deformation splitting of E1 GR is practically a single *direct* manifestation of quadrupole prolate and oblate deformation in clusters.

3) Like in atoms, the spin-orbit interaction in MC is negligible and the spin and orbit collective modes are well decoupled. As a result, the investigation of orbital collective modes in MC is much easier than in nuclei. This feature is important also for application of fluid-dynamical and self-consistent models which, as a rule, do not take into account spin degrees of freedom.

4) In nuclei, the investigation of collective excitations is often complicated by the need to restore the translational and rotational invariances violated by the model Hamiltonian. In MC, the mass of valence electrons is much smaller than the mass of ions and, as result, the problem of restoration of translational and rotational invariances is not so important.

5) Physical interpretations of E1 GR in MC and nuclei are very similar: E1 GR in nuclei is caused by the out-of-phase translations of neutron and proton subsystems while E1 GR in MC is a result of the translations of the valence electron subsystem with respect to the ionic subsystem. In spite of this similarity, the E1 GR energy in MC increases with  $N$ , in contrast with the  $A^{-1/3}$  dependence in nuclei. Indeed, within the SRM, the energy of E1 GR in MC is written as  $\omega = \sqrt{\frac{4\pi}{3}n} \left\{ 1 - \frac{1}{2} \frac{\delta N_e}{N_e} \right\}$  where  $\delta N_e = \int_{r>R} dr n_0(r)$  is the number of valence electrons outside the radius  $R$  specified by the ionic jellium (the so called "spill-out" electrons) and  $n_0(r)$  is the density of valence electrons. The larger the "spill-out" effect, the smaller the energy of the E1 GR. Since the number of the "spill-out" electrons decreases with  $N$ , we have the corresponding increase in the E1 excitation energy. The "spill-out" effect plays a crucial role in the description of EL GR in MC [2-5,7].

6) As has been shown in [17], the fragmentation of the E1 GR in MC depends strongly on the cluster's charge. Being the strongest in negatively charged clusters, the fragmentation is drastically reduced when passing to neutral and then to positively charged clusters. This effect provides the chance to investigate E1 GR under quite favorable conditions of minimal fragmentation.

Let us consider the results of calculations for E1 and E2 GR, obtained within the VPM. Being widely used in nuclear physics (see, i.e., [18-22], this model was modified for MC in [23] and then generalized to the description

of GR in clusters of any shape in [7,24,25]. The VPM is the self-consistent version of the schematic RPA with a separable residual interaction. The self-consistency condition between variations of the ground state density and the single-particle potential provides the form of residual forces and the analytical expression for their strength constants. Being the self-consistent microscopical model, the VPM, nevertheless, does not need time consuming calculations.

For the external field  $f_{\lambda\mu}(\vec{r}) = r^\lambda Y_{\lambda\mu}^d(\Omega)$  corresponding to irrotational and divergency free collective motion (here,  $Y_{\lambda\mu}^d(\Omega) = Y_{\lambda\mu}(\Omega) + d \cdot Y_{\lambda\mu}^\dagger(\Omega)$ ,  $Y_{\lambda\mu}(\Omega)$  is a spherical harmonic and  $d = \pm 1$ ), the main VPM equations are written as [7,23-25]

$$H = \bar{H}_0 - 1/2 \sum_{\lambda\mu} \kappa_0^{(\lambda\mu)} Q_{\lambda\mu}(\vec{r}) Q_{\lambda-\mu}(\vec{r}), \quad (1)$$

$$Q_{\lambda\mu}(\vec{r}) = \vec{\nabla} V_0(\vec{r}) \cdot \vec{\nabla} f_{\lambda\mu}(\vec{r}) + \int \frac{\vec{\nabla} n_0(\vec{r}_1) \cdot \vec{\nabla} f(\vec{r}_1)}{|\vec{r} - \vec{r}_1|} d\vec{r}_1, \quad (2)$$

$$(\kappa_0^{(\lambda\mu)})^{-1} = - \int Q_{\lambda\mu}(\vec{r}) \vec{\nabla} f_{\lambda\mu}(\vec{r}) \cdot \vec{\nabla} n_0(\vec{r}) d\vec{r} \quad (3)$$

and

$$X_{\lambda\mu} \equiv 2 \sum_{kk'} \frac{\langle k' | Q | k \rangle >^2 (\epsilon_k + \epsilon_{k'})}{(\epsilon_k + \epsilon_{k'})^2 - \omega_{\lambda\mu}^2} = (\kappa_0^{(\lambda\mu)})^{-1} \quad (4)$$

where the ground state density of the valence electrons is calculated as  $n_0(\vec{r}) = \sum_k | | k > |^2$ ,  $| k >$  and  $\epsilon_k$  are the single-particle eigenstate and eigenenergy of the static single-particle hamiltonian  $H_0$  and  $\omega_l$  is the root of equation (4). Eqs. (1)-(4) describe the Hamiltonian, the residual forces, the inverse strength constant of these forces and the dispersion equation, respectively. If the Coulomb term in (2) is neglected, we have the VPM equations for isoscalar  $E\lambda$  GR in atomic nuclei [21,22,24]. So, the VPM is suitable for studying  $E\lambda$  GR in both MC and nuclei [24].

In Figs. 1-3 the results of the VPM calculations for E1 and E2 GR in deformed sodium clusters (oblate  $Na_{18}$  and prolate  $Na_{26}$ ) are presented [25]. The calculations have been performed with the Woods-Saxon single-particle potential

$$V_0(\vec{r}) = \frac{U_0}{1 + \exp[(r - R(\Omega))/a_0]} \quad (5)$$

with  $R(\Omega) = R_0(1 + \beta_0 + \beta_2 Y_{20}(\Omega) + \beta_4 Y_{40}(\Omega))$ ,  $R_0 = r_0 N_c^{1/3}$  and values of the parameters  $U_0 = -6\text{eV}$ ,  $r_0 = 2.25\text{\AA}$  [11] and  $a_0 = 1.0\text{\AA}$  [25]. Following [26], the parameters of quadrupole and hexadecapole deformation were taken to be equal to  $\beta_2 = -0.23$  and  $\beta_4 = 0.02$  for oblate  $Na_{18}$  and  $\beta_2 = 0.40$  and

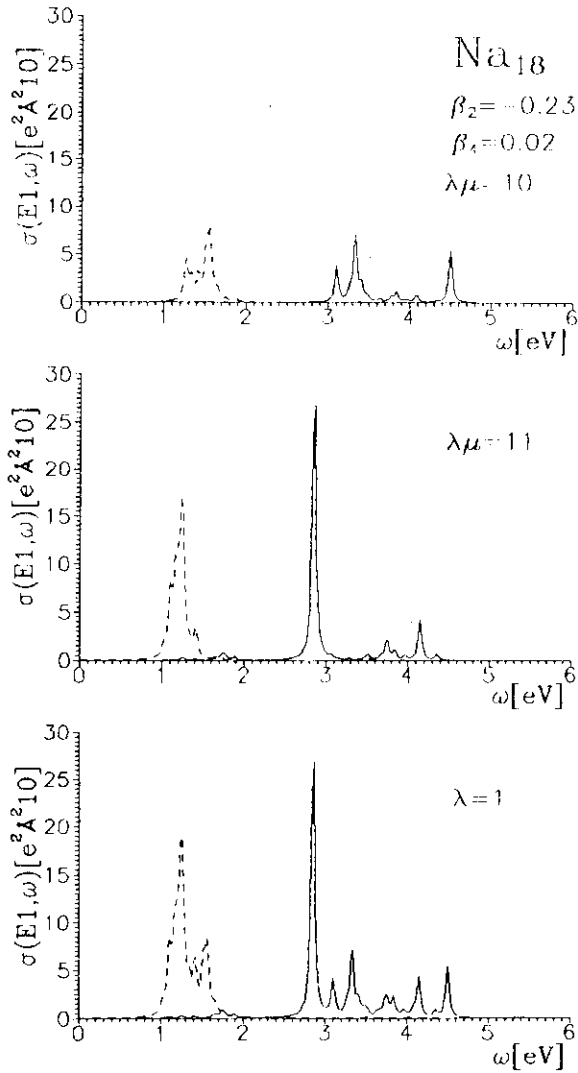


Fig.1 The strength function  $\sigma(E1, \omega) = b_1(E1, \omega)$  for E1 excitations in  $\text{Na}_{18}$  [25]. The plots are given for each projection  $\mu = 0, 1$  and for the total case (bottom). Solid and dashed lines represent the results obtained with and without the residual interaction, respectively.

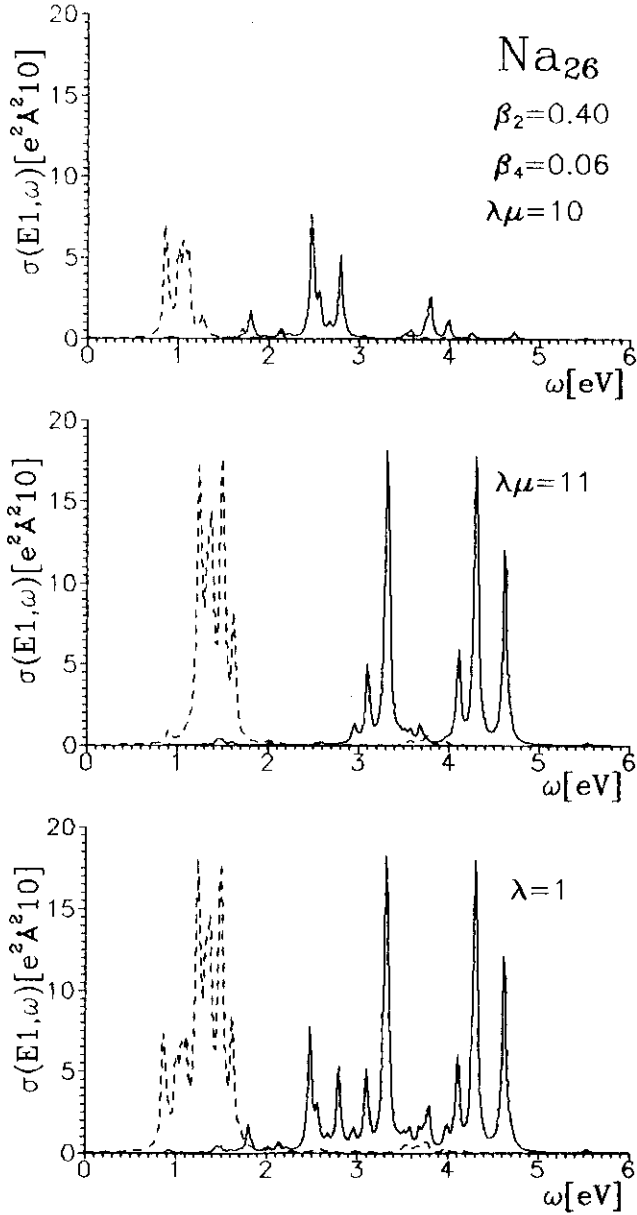


Fig.2 The same as in Fig.1 for  $\text{Na}_{26}$  [25].



$\beta_4 = 0.06$  for prolate  $Na_{26}$ . The results in Figs. 1-3 are presented in the form of the strength function [25]

$$b_m(E\lambda\mu, \omega) = \sum_t \omega_t^m B(E\lambda\mu, gr \rightarrow \omega_t) \rho(\omega - \omega_t) \quad (6)$$

with the weight factor  $\rho(\omega - \omega_t) = \frac{1}{2\pi} \frac{\Delta}{(\omega - \omega_t)^2 + (\Delta/2)^2}$ . Here,  $B(E\lambda\mu, gr \rightarrow \omega_t)$  is the reduced probability of the  $E\lambda\mu$  transition from the ground state to the one-phonon state  $\omega_t$ ,  $\Delta$  is the averaging parameter (to be equal to 0.05eV in the present calculations).

The results for E1 excitations are depicted in Figs.1 and 2. The strength function  $b_1(E1\mu, \omega)$  is given for two cases: with and without the residual interaction. In the latter case,  $\kappa_0^{(\lambda\mu)} = 0$  and E1 excitations are determined by particle-hole transitions of noninteracting valence electrons. Then, the E1 resonance is localized in the region 0.8-1.8 eV that is much lower than the experimental values (experimental data [27] exhibit the two peak structure with the energies 2.56 and 2.94 for  $Na_{18}$  and 2.29 and 2.93 eV for  $Na_{26}$ ). The energy 0.8-1.8 eV is a typical energy interval between neighbour shells. This interval corresponds to E1 transitions with  $\Delta N_{sh} = 1$  where  $N_{sh}$  is the principal shell quantum number. The self-consistent residual interaction shifts the resonance towards the energy 2.6-3.3 eV which is in accordance with the experimental values. As is seen from the Figs.1 and 2, the deformation of clusters leads to the same picture as in atomic nuclei. Namely, in prolate  $Na_{26}$ , the small peak corresponding to vibrations of electrons along the z-axis of the spheroid has lower energy as compared with the large peak corresponding to vibrations of electrons along the x- and y-axes. In oblate  $Na_{18}$ , the opposite picture takes place. Due to the deformation splitting, resonances in  $Na_{18}$  and  $Na_{26}$  demonstrate the substantial Landau damping. The experimental deformation splitting is well reproduced although this is mainly a merit of the single-particle scheme. The analysis of the structure of the main peaks shows that these peaks are composed from many particle-hole excitations, i.e., have a collective nature.

Figs.1 and 2 show that E1 excitations have pronounced high-energy peaks which are well separated from the main E1 resonance. These peaks exhaust a large amount, up to 30%, of the model-independent energy-weighted sum rule which somewhat overestimates the experimental value 10–20%. In spite of this discrepancy, the existence of the high-energy peaks seems to be reasonable. This is a peculiarity of MC that the long-range Coulomb forces promote the interaction between remote electrons and thus favour  $\Delta N_{sh} = 3, 5, \dots$  transitions and formation of the high-energy peaks. The high-energy strength seems to be maximal in clusters of a moderate size (from tens to several hundred of atoms). Small clusters have not enough number of shells to provide noticeable high-energy strength. On

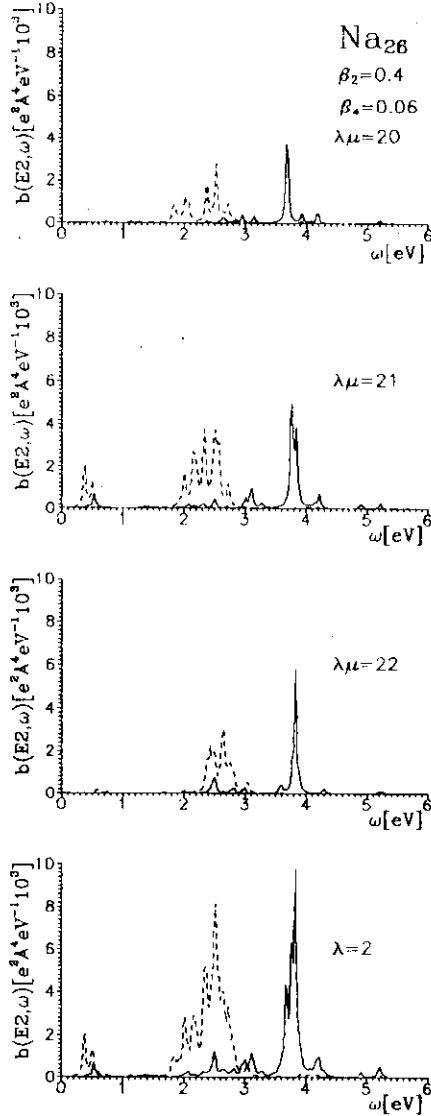


Fig.3 The strength function  $b(E2, \omega) \equiv b_0(E2, \omega)$  for E2 excitations in  $\text{Na}_{26}$  [25]. The plots are given for each projection  $\mu = 0, 1, 2$  and for the total case (bottom). Solid and dashed lines represent the results obtained with and without the residual interaction, respectively.

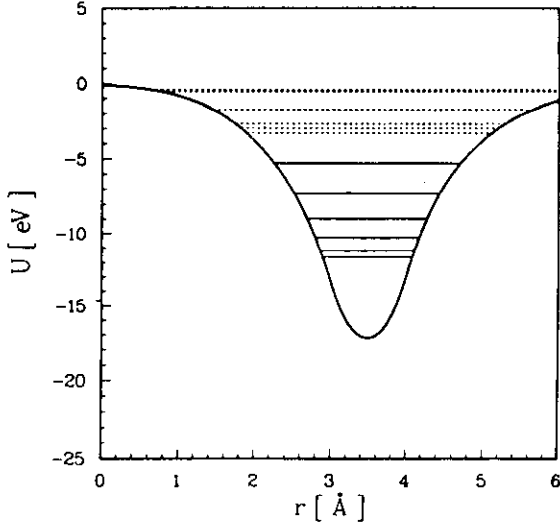


Fig.4 The single-particle potential in  $C_{60}$  [36].

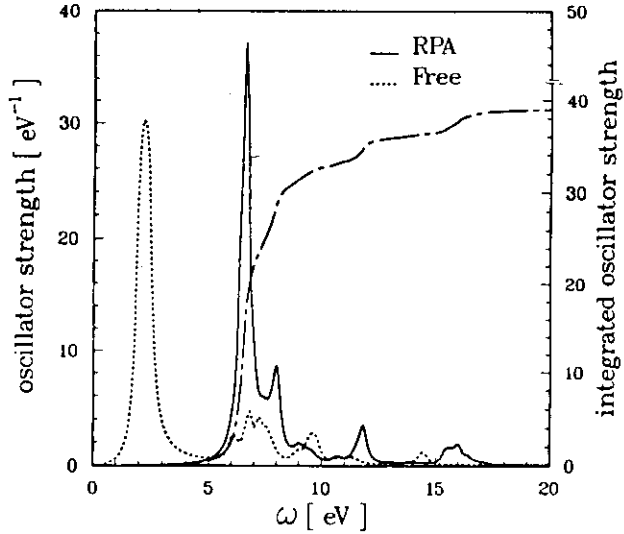


Fig.5 The E1 GR formed by the  $\pi$ -electrons in  $C_{60}$ . The calculations have been performed within the RPA [36].

the other hand, in very large clusters the energy intervals between shells are too small to result in any sizable  $\Delta N_{sh}$  effects.

In Fig. 3, the strength functions  $b_0(E2\mu, \omega)$  for E2 excitations in  $Na_{26}$  are presented [25]. For the first time, the calculations were performed by taking into account the fragmentation of the E2 strength. It is seen that the unperturbed (particle-hole) E2 excitations are mainly formed by  $E2(\Delta N_{sh} = 2)$  transitions with the energy about 2 eV. The residual interaction shifts the strength to the energy 3.5 eV. The important point is that E2 GR is not much fragmented so that this GR has a good chance to be measured in the  $(e, e')$  reaction.

We see that, in spite of numerous interesting peculiarities mentioned in the onset of this subsection,  $E\lambda$  GR in MC and atomic nuclei are rather similar. One can expect more differences for orbital  $M\lambda$  GR. In MC, the decoupling of orbital and spin degrees of freedom and possibility to get considerable orbital moments in large clusters can lead to a new interesting physics. The fluid-dynamical models derived in nuclear physics (see, e.g. [7,28-32]) can be effectively used in this field.

## 4 Fullerenes, helium clusters and quantum dots

Let us briefly consider other members of the SFS family: fullerenes,  $^3He$  and  $^4He$  clusters and quantum dots.

**Fullerenes.** About ten years ago a unique experimental technique was developed to produce atomic clusters of virtually any element of the Mendeleev's table. The most surprising results were obtained for carbon. It turned out that beginning from  $N=40$  only clusters with an even number of atoms are stable. These carbon clusters have been named fullerenes. The cluster  $C_{60}$  turned out to be especially stable, which allowed one to consider  $N=60$  as a magic number and to announce  $C_{60}$  as a fourth state of carbon together with diamond, soot and graphite. This cluster has the exotic form of a football, i.e., of a sphere with the radius of  $4\text{\AA}$  and with the  $3\text{\AA}$  hole inside. The general information about fullerenes can be found in refs. [1,33-35].

The carbon atom has four valence electrons: three with strong  $\sigma$  bounds and one with a weaker  $\pi$  bond. In  $C_{60}$ , the  $\pi$ -electrons form a subsystem of 60 interacting electrons. They determine such important properties of the fullerene as ionization potential and conductivity. In analogy with MC, the rest ionic subsystem of  $C_{60}$  (including the 180 deeply bound  $\sigma$  electrons) can be considered in a good approximation as a uniformly charged jellium. The external ionic potential and the interaction between  $\pi$ -electrons create the self-consistent mean field for the 60  $\pi$ -electrons. This mean field is exhibited in Fig.4 [36].

Collective translations of the  $\pi$ -electrons with respect to the ionic jellium form E1 GR. This GR has recently been observed in crystalline  $C_{60}$  around 6-7 eV exhausting about 1/2 of the integrated  $\pi$  oscillator strength [37,38]. Besides the E1 GR formed by the  $\pi$ -electrons, another broad resonance at about 25 eV has been observed and interpreted as the E1 GR formed by all the valence electrons ( $\pi + \sigma$  electrons). This resonance has also been observed at about 20 eV in photon ionization experiments on free  $C_{60}$  [39].

Both the  $\pi$  and  $\pi + \sigma$  E1 GR have been calculated within different approaches widely used in nuclear theory: SRM and RPA (see, for example, [36,40,41]). The results of the RPA calculations for the  $\pi$  E1 GR are presented in Fig.5 [36]. It is interesting that these results practically do not depend on the thickness of the  $C_{60}$  sphere. This means that the  $\pi$  E1 GR is mainly of the surface nature. It is worth noting also a large amount, up to 33%, of the "spill-out" electrons in  $C_{60}$  [36].

Fullerenes attract much attention now. To a large extent, this is connected with possible new carbon-based technologies (fullerene-encapsulated atoms, doped fullerene cages, buckytubes, superconductors, buckyfibers, etc., [35]) and with the observation of the high-temperature superconductivity (18-28 K) in the metals obtained by doping  $C_{60}$  with alkali atoms (see, e.g., [42]).

**Helium clusters.** There are two kinds of helium clusters: (a) collections of  ${}^3He$  atoms, i.e., of fermions, and (b) collections of  ${}^4He$  atoms, i.e., of bosons [1,6,43]. Helium atoms form a self-consistent field with the corresponding shell structure. For example, in  ${}^3He$  droplets the shell closures agree with the harmonic oscillator scheme up to  $N=168$  [6,44]. Unlike MC and fullerenes, the particles moving in a mean field of helium clusters are not valence electrons but helium atoms. The experimental investigation of helium clusters is still in its infancy. The main trouble is that helium clusters are very weakly bound (for example, the binding energy is about 1.5 K (or  $10^{-4}$  eV) in  ${}^3He$  clusters and still less in  ${}^4He$  clusters) which makes their ionization and subsequent detecting very difficult. So, our present knowledge of helium clusters, including their shell structure, is based on theoretical studies.

The mean field of helium clusters is obtained in close similarity with the Hartree-Fock mean field calculated in atomic nuclei on the basis of the Skyrme functional. For example, in [6,44] the self-consistent mean field of  ${}^3He$  clusters was obtained in the framework of the recently developed effective energy functional employing a realistic finite range interaction between helium atoms. In [45,46], the starting point for the mean field was the effective  ${}^3He - {}^3He$  interaction proposed in [47]. This mean field

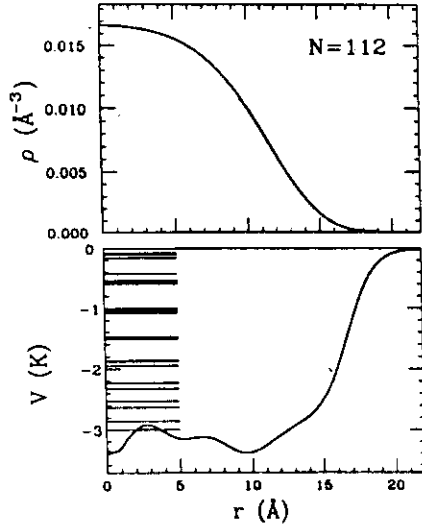


Fig.6 The calculated self-consistent mean field and corresponding particle density in  ${}^3\text{He}$  cluster with  $N=112$  atoms [45].

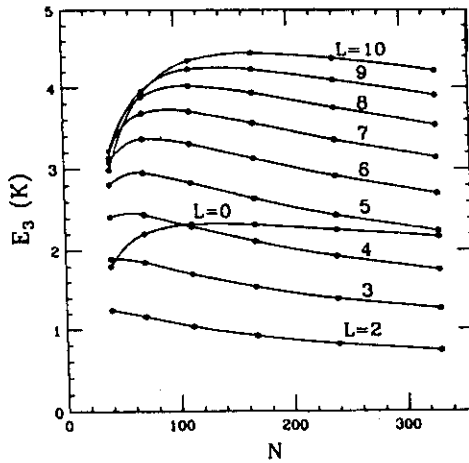


Fig.7 The excitation energies of the E0 and E2-E10 GR in  ${}^3\text{He}$  clusters, calculated within the SRM [45].

together with the corresponding particle density is presented in Fig.6 [45]. It is seen that the single-particle potential in helium clusters has very large diffuseness. The surface effects in  ${}^3\text{He}$  clusters are so large that the clusters need several thousand atoms in order to reduce, for example, the surface contribution to the mass formula to about 10% [43].

The E1 GR is absent in helium clusters since this system consists of particles of one sort. For calculations of  $E\lambda(\lambda = 0, 2, 3, \dots)$  GR, SRM and RPA are again used [6,44-46,48]. In Fig.7, the results of calculations within the SRM for E0 and E2-E10 GR in  ${}^3\text{He}$  clusters are presented [45].

As compared with atomic nuclei, MC and fullerenes, the study of GR in helium clusters reveals at least four new possibilities: (i) the comparison of GR in quantum systems with fermion and boson statistics, (ii) the peculiarities of GR in a one-component quantum system, (iii) the study of GR in very large quantum systems (one can produce helium clusters with the number of atoms  $N > 10^5$ ) and (iiii) the study of GR in systems with strong surface effects.

Besides GR, there are other interesting branches of the helium-cluster physics. First of all, investigation of the difference between  ${}^3\text{He}$  and  ${}^4\text{He}$  clusters, caused by different quantum statistics. It is known, for example, that  ${}^4\text{He}$  clusters are always bound while  ${}^3\text{He}$  clusters need a minimum number of atoms (about  $N=30$ ) to give binding. Other interesting problem is connected with possible superfluidity in helium clusters.

**Quantum dots.** Modern experimental technique allows one to create at a semiconductor interface (by periodic etching or gating) little quasi-two-dimensional disks, typically  $\sim 1000\text{\AA}$  in diameter and confining 2-200 electrons (see, e.g., [8]). At sufficiently low temperatures, the mean free path of these electrons is larger than the disk diameter, thus leading to quantization of the system. These structures are called quantum dots. Clearly, they can be considered as two-dimensional clusters [2].

Quantum dots exhibit E1 GR as translations of electrons with respect to the disk. The essential feature of E1 GR in a quantum dot is that its excitation energy does not depend on the number of electrons, i.e., is not influenced by the electron-electron interaction [49]. This rather surprising feature is explained by the fact that the single-particle potential confining electrons is of the harmonic oscillator form in the  $x - y$  plane. It can be shown that, if the Hamiltonian consists of the oscillator mean field and the residual interaction (which depends only on the relative distance between electrons, the Coulomb interaction in our case), then the system will absorb light only at the oscillator frequency [50-52]. This rule has been generalized in [51] for the presence of the magnetic field as well: the resonance frequencies in the magneto-optical absorption spectrum of a quantum dot

with parabolic confinement are independent of the electron-electron interaction and are given by the single-electron transition frequencies. The calculations for E1 GR in [50-52] have been performed within the RPA.

## 5 Conclusions

The new family of SFS (metal clusters, fullerenes,  $^3He$  and  $^4He$  clusters and quantum dots) discovered about ten years ago increases much our possibilities for investigation of both general and particular properties of Fermi systems. Together with nuclei and atoms we have now a wide variety of SFS:

- with strong (nuclei) and Coulomb (atoms and new SFS) interaction; consisting of fermions and bosons ( $^3He$  and  $^4He$  clusters);
- two-dimensional (quantum dots) and three-dimensional (other SFS);
- with very large numbers of particles (MC and helium clusters);
- with moderate (nuclei, MC) and strong (helium clusters) diffuseness of the surface;
- saturated (nuclei and MC) and with behavior of quantum gas (atoms);
- of exotic form ( $^{60}C$ );
- one-component (helium clusters) and two-component (other SFS).

All these SFS have a common property: the mean path of their particles is of the same order as the size of the system, which creates conditions for quantization of the system and forming the mean field like in atomic nuclei. Except atoms, all these systems possess the saturation property (nearly constant density). This allows one to use for their study the powerful potential of nuclear theoretical physics.

This talk is only a brief sketch of the properties of the new SFS with the aim to present the first information and to attract attention to this really exciting field. We believe that the appearance of the new family of the SFS as well as the possibility to use for their investigation the large experience of nuclear physics provide very favourable conditions for investigation of fundamental properties of Fermi systems and will lead to discoveries of fundamental character. The discovery of supershells is the first example.

It should also be mentioned, that new SFS are very promising for practical applications. There are interesting possibilities for aerosols, powder technologies, catalysis, superconductivity, etc.. The nanometer size of the new SFS is typical of the modern microelectronics.

## REFERENCES

1. Bjornholm, S.: Contemp.Phys. **31**, n.5 309 (1990)



2. Kresin, V.V.: Phys.Rep. **220**, 1 (1992)
3. Nesterenko, V.O.: Sov.J.Part.Nucl. **23**, 1665 (1992)
4. de Heer, W.A.: Rev.Mod.Phys. **65**, 611 (1993)
5. Brack, M.: Rev.Mod.Phys. **65**, 677 (1993)
6. Weisgerber, S. and P.-G. Reinhard: Ann.Physik **2** 666 (1993)
7. Nesterenko, V.O., Kleinig, W. and Shirikova, N.Yu.: Izv.Akad.Nauk, ser.fiz., **58**, 16 (1994)
8. Proc. 8th Int.Conf. on Electronic Proper. of Two-Dimens. Systems -- Surf.Sci. **229** (1990)
9. Brechignac, C. and Connerade, J.P.: J.Phys.B **27** 3795 (1994)
10. Balian, R. and Bloch, C.: Ann.Phys. **69** 76 (1971)
11. Nishioka, H., Hansen, Kl. and Mottelson, B.R.: Phys.Rev. **B42** 9377 (1990)
12. Pedersen, J. et al: Nature **353** 733 (1991)
13. Frauendorf, S. and Pashkevich, V.V.: Z. Phys. **D26**, S-98 (1993)
14. Frauendorf, S. and Pashkevich, V.V.: Preprint FZR-37, Rossendorf, 1994, submit. to Phys.Rev.B.
15. Kuzmenko, N.K., Nesterenko, V.O., Frauendorf, S. and Pashkevich, V.V.: Preprint JINR E4-94-525, Dubna, 1994
16. Clemenger, K.: Phys.Rev. **B32** 1359 (1985)
17. Yannouleas, C.: Chem.Phys.Lett. **193** 587 (1992)
18. Rowe, D.J.:In: Nuclear Collective Motion, Methuen, London, 1970
19. Bohr, A. and Mottelson, B.R.:In: Nuclear Structure, v.2, Benjamin, New-York, 1975
20. Suzuki, T. and Rowe, D.J.: Nucl.Phys. **A289**, 461 (1977)
21. Lipparini, E. and Stringari, S.: Nucl.Phys. **A371**, 430 (1981)
22. Nesterenko, V.O., Kleinig, W., Gudkov, V.V. and Kvasil J.: Preprint JINR E4-95-201, Dubna (1995)
23. Lipparini, E. and Stringari, S.: Z.Phys. **D18**, 193 (1991)

24. Nesterenko, V.O. and Kleinig: Phys.Scr. (1995), in press.
25. Nesterenko, V.O., Kleinig, W. and Gudkov, V.V.: Preprint JINR E4-94-510, Dubna, 1994; Z.Phys.D (1995) in press
26. Hirschmann, Th., Brack, M. and Mejer, J.: Annalen Physik **3**, 336 (1994)
27. Selby, K. et al.: Phys.Rev. **B40**, 5417 (1989)
28. Holzwarth, G. and Eckart, G.: Nucl.Phys. **A325** 1 (1979)
29. Nix, J.R. and Sierk, A.J.: Phys.Rev. **C21** 396 (1980)
30. Stringari, S.:Ann.Phys. **151** 35 (1983)
31. Bastrukov, S.I. and Gudkov, V.V.: Z.Phys.A **341** 395 (1992)
32. da Providencia, J. and de Haro, Jr.R.: Phys.Rev. **B49**, 2086 (1994)
33. Kroto, H.W. and McKay, K.: Nature **331** 328 (1988)
34. Curl, R.F. and Smalley, R.E.: Sci. Am. **265** 54 (1991)
35. Smalley, R.E.: Acc. Chem. Res. **25**, n.3, 98 (1992)
36. Nguen Van Giai and Lipparini, E.: Z.Phys.D **27** 193 (1993)
37. Sohmen, E., Fink J. and Kratschmer, W.: Europhys. Lett. **17** 51 (1992); Z.Phys.B **86** 87 (1992) and ref. therein.
38. Gensterblum, G. et al: Phys.Rev.Lett. **67** 2171 (1991)
39. Hertel, I.V. et al: Phys.Rev.Lett. **68** 784 (1992)
40. Yabana, K. and Bertsch, G.F.: Phys.Scr. **48** 633 (1993)
41. Broglia, R.A. et al: Z.Phys.D **31** 181 (1994)
42. Zhang, F.C. et al: Phys.Rev.Lett. **67** 3452 (1991)
43. Stringary, S.: Z.Phys.D **20** 219 (1991)
44. Weisgerber, S. and P.-G. Reinhard: Z.Phys.D **23** 275 (1992)
45. Serra, Ll. et al: Z.Phys.D **20** 277 (1991)
46. Serra, Ll. et al: Phys.Rev.Lett. **67** 2311 (1991)
47. Stringary, S.: Phys.Lett. **A107** 36 (1985)
48. Casas, M. and Stringary, S.: J.Low.Temp.Phys. **79** 135 (1990)

49. Sikorski, Ch. and Merkt, U.: Phys.Rev.Lett. **62** 2164 (1989)
50. Brey, L., Johnson, N.F. and Halperin, B.I.: Phys.Rev. **B40** 10647 (1989)
51. Peeters, F.M.: Phys.Rev. **B42** 1486 (1990)
52. Shikin, V.: Phys.Rev. **B43** 11903 (1991)

Received by Publishing Department  
on May 12, 1995.